

# Coherent control near metallic nanostructures

Ilya Grigorenko

*Theoretical Division T-17, Center for Nonlinear Studies, Center for Integrated Nanotechnologies,  
Los Alamos National Laboratory, Los Alamos, New Mexico 87545, USA*

Anatoly Efimov

*Center for Integrated Nanotechnologies, Los Alamos National Laboratory, Los Alamos, New Mexico 87545, USA*

(Dated: August 5, 2008)

We study coherent control in the vicinity of metallic nanostructures. Unlike in the case of control in gas or liquid phase, the collective response of electrons in a metallic nanostructure can significantly enhance different frequency components of the control field. This enhancement strongly depends on the geometry of the nanostructure and can substantially modify the temporal profile of the local control field. The changes in the amplitude and phase of the control field near the nanostructure are studied using linear response theory. The inverse problem of finding the external electromagnetic field to generate the desired local control field is considered and solved.

Last two decades have witnessed the birth and rapid progress in manipulation of quantum systems, such as atoms and molecules [1, 2, 3], semiconductor quantum dots [4] or even complex biological systems [5] by means of optimally shaped ultrashort laser pulses. Coherent control is usually achieved in homogeneous gas or liquid phase by the direct coupling of electronic or molecular degrees of freedom of the system being controlled to the external electromagnetic fields. However, it is known that most of the important chemical reactions in nature and technology take place at surfaces or interfaces. For example, at the surface of a catalyst (usually metal) breaking and formation of chemical bonds takes place on a femtosecond time scale and observation of the dynamics can be performed, e.g., using a pump-probe technique [6]. The induction and control of chemical reactions, such as oxidization of CO on a metal surface, using ultrashort laser pulses is very important from scientific and technological points of view [7, 8].

For coherent control of atoms or molecules near metallic surfaces, metallic clusters or other nanostructures the situation becomes very different from the control in homogeneous dielectric media. The interaction of valence electrons with external field may lead to collective, geometry-dependent excitation modes and produce local fields few orders of magnitude larger than the incident control field [9]. In this case the direct coupling of the control field to the controlled molecule may be much weaker than indirect coupling via interaction with the excited plasmon modes. Note, that one has to distinguish between the static spatial localization of the induced field near sharp edges of metallic nanostructure and excitation of spatially localized plasmonic modes. The interaction of electromagnetic field with a metallic nanostructure, unlike in the case of homogeneous dielectric medium, creates highly inhomogeneous induced local field distribution. The spatial variations of the field intensity may be significant on a scale as small as one nanometer [9]. The effect of the presence of a metallic nanostructure is

not limited to the local field enhancement only, but may also result in the broadening of a state linewidth in a quantum system due to dynamical screening effects. For example, recent measurements demonstrate [10] reduction of fluorescence lifetime of dye molecules (from 2.8 ns to less than 1 ns) in the presence of nanostructured metal surface.

Since *ab initio* simulations of a controlled quantum system and electrons in the nanostructure may be computationally extremely expensive, most of the previous modeling of temporal characteristics of the local fields and associated quantum dynamics was typically performed for oversimplified models, with the focus on some particular aspects of the problem. For example, a quantum mechanical treatment of time-dependent screening and associated transient effects due to sudden creation of a charge in a close vicinity of two dimensional electron gas, was considered in [11]. Other simulations, involving more realistic geometries than an idealized two-dimensional electron gas, are usually performed using classical Finite Difference Time Domain (FDTD) approach. One can mention coherent control of nanoscale localization of optical excitations in nanosystems [9], where classical equations with local phenomenological dielectric constant  $\epsilon(\mathbf{r})$  were used. However, the validity of local classical response theory is questionable for relatively small or highly inhomogeneous nanostructures, where quantum mechanical effects may play a critical role. In the quantum limit one needs to take into account the discreteness of the energy spectrum, non-local electron density response, dynamical screening effects and tunneling [12].

As can be seen, the coherent control of atoms and molecules localized near metallic nanostructures is much more complex than in a gas or liquid phase. It is important for the theory to capture the fact that the incident electromagnetic field is coupled both to single particle and collective plasma excitations in the nanostructure, and the field in the nanostructure is neither completely screened, nor purely transverse. To develop the theory

of the coherent control at the nano (i.e. subwavelength) scale, we need to map out spatio-temporal or spatio-spectral amplitude as well as the phase of the local field in relation to the external spatially-uniform, but temporally shaped excitation field. More importantly, the inverse problem of finding the external field corresponding to the required local control field for the best performance needs to be addressed. It may seem that the modification of the control field in the vicinity of a metal nanostructure makes coherent control very difficult or impossible. However, we will show that one can successfully generate local control fields with the prescribed temporal behavior and take advantage of local field enhancement.

In this study we consider the problem of coherent control in the presence of a doped semiconductor nanostructure and propose to use the local field enhancement due to geometrical and resonant plasmon excitation for optimal control of atoms and molecules. Relatively long relaxation and dephasing times were reported for heavily doped semiconductor heterostructures [13]. The carrier concentration in the nanostructure is chosen to generate plasmon resonance around 0.8 eV, which corresponds to the wavelength  $\lambda = 1550$  nm. The experimental techniques for generation, shaping and detection of ultrashort pulses at this wavelength are readily available. Also, this wavelength range is important for excitation and optimal control of molecular wave packet formation using a two-color pump-probe scheme [14]. The Fermi wavelength at this carrier concentration is  $\approx 10$  nm, comparable to the size of the nanostructure (several tens of nanometers within capabilities of modern nanofabrication methods), which motivates us to use quantum nonlocal linear response theory [12]. Using the theory [12], we examine the inhomogeneous distribution of the induced field, and study how the control pulse intensity and phase are transformed due to the plasmonic response of a small custom-engineered nanostructure.

In the self-consistent treatment the induced charge density in the nanostructure  $\rho_{\text{ind}}(\mathbf{r}, t)$  is given by:

$$\rho_{\text{ind}}(\mathbf{r}, t) = \int_{-\infty}^{+\infty} dt' \int d\mathbf{r}' \chi_0(\mathbf{r}, \mathbf{r}', t, t') \phi_{\text{tot}}(\mathbf{r}', t'), \quad (1)$$

where  $\phi_{\text{tot}}(\mathbf{r}, t) = \phi_{\text{ext}}(\mathbf{r}, t) + \phi_{\text{ind}}(\mathbf{r}, t)$  is the total potential, and  $\chi_0(\mathbf{r}, \mathbf{r}', t, t') = -\theta(t - t') < \rho(r, t), \rho(r', t') >_0$  is the electron polarizability, and the statistical average is performed over the equilibrium state. The function  $\theta(t - t')$  ensures the causality of the electron response.

We assume the density-density response function is translation invariant in time variables  $\chi_0(\mathbf{r}, \mathbf{r}', t, t') \equiv \chi_0(\mathbf{r}, \mathbf{r}', t - t')$ , but not in the space variables. By making Fourier transform in time domain and assuming Random Phase Approximation (RPA), one can express  $\chi_0(\mathbf{r}, \mathbf{r}', \omega)$  in terms of the eigenenergies and eigenfunctions of the the

unperturbed Hamiltonian:

$$\chi_0(\mathbf{r}, \mathbf{r}', \omega) = \sum_{i,j} \frac{f(E_i) - f(E_j)}{E_i - E_j - \hbar\omega - i\gamma} \psi_i^*(\mathbf{r}) \psi_i(\mathbf{r}') \psi_j^*(\mathbf{r}') \psi_j(\mathbf{r}), \quad (2)$$

where  $f$  is the Fermi distribution function, and  $\gamma$  accounts for the finite width of the quantum levels in the nanostructure. The eigenproblem for electrons confined in the nanostructure  $H\psi_i(\mathbf{r}) = E_i\psi_i(\mathbf{r})$  is solved using numerical diagonalization.

The induced potential  $\phi_{\text{ind}}(\mathbf{r}, \omega)$  is determined from the self-consistent integral equation [12]

$$\phi_{\text{ind}}(\mathbf{r}, \omega) = \int \int \chi_0(\mathbf{r}', \mathbf{r}'', \omega) \phi_{\text{tot}}(\mathbf{r}'', \omega) V_C(|\mathbf{r} - \mathbf{r}'|) d\mathbf{r}' d\mathbf{r}'', \quad (3)$$

where  $V_C(|\mathbf{r} - \mathbf{r}'|)$  is the Coulomb potential. Here we make use of the fact that the nanostructure is much smaller than the wavelength of the incoming field, so the retardation effects can be neglected. In order to find  $\phi_{\text{ind}}(\mathbf{r}, \omega)$  we discretize Eq.(3) on a real-space cubic mesh and solve it numerically. The equation Eq.(3) establishes one-to-one correspondence between the homogeneous external control field  $\mathbf{E}_{\text{ext}}(\omega)$  and the total (local) field  $\mathbf{E}_{\text{tot}}(\mathbf{r}, \omega)$  at a given point  $\mathbf{r}$ . Note that this correspondence is established using statistical average and has no uncertainties related to quantum dynamics of electrons for nanostructures with large number of electrons.

Since we work in a weak-field limit and assume linear response of the system, there is no mixing or creation of new frequency components, which were not originally present in the incoming control field. This linear response approximation significantly simplifies the analysis in that the response of the system can be computed for each frequency separately in the spectral domain:

$$\mathbf{E}_{\text{tot}}(\mathbf{r}_0, \omega) = \hat{\mathbf{Z}}(\mathbf{r}_0, \omega) \mathbf{E}_{\text{ext}}(\omega), \quad (4)$$

where  $\mathbf{r}_0$  is the position of the controlled molecule, and for a small metallic nanostructures the complex valued local response kernel  $\hat{\mathbf{Z}}(\mathbf{r}_0, \omega)$  is non-zero for any  $\omega$ . Thus, the expression Eq.(4) can be inverted, and the optimal external field can be computed given the required local control field  $\mathbf{E}_{\text{tot}}(\mathbf{r}_0, \omega)$ .

To illustrate our approach we consider a finite nanostructure with dimensions  $L \times L \times d$ ,  $L = 33$  nm,  $d = 10$  nm, made of a doped semiconductor with the carrier concentration  $n = 9.5 \times 10^{19} \text{cm}^{-3}$  with a bow-tie shaped hole, Fig.1(a). Nanostructures of such shape are routinely manufactured for local field enhancement [15]. There are total 1042 electrons confined in the nanostructure. The electron effective mass is taken to be  $0.2m_e$ , where  $m_e$  is the bare electron mass [16]. The carrier concentration is chosen to generate plasmon resonance around 0.8 eV.

In our simulations we set the phenomenological damping parameter to  $\gamma = 3.8$  meV [13]. We performed

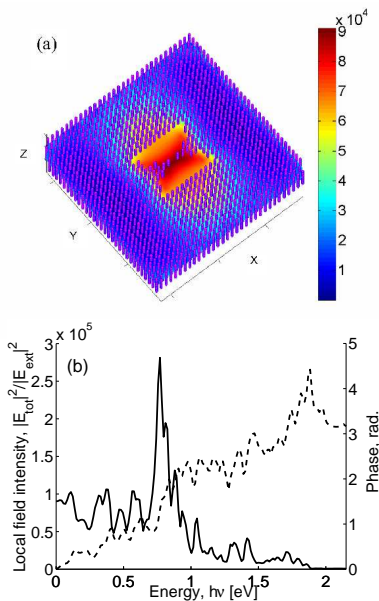


FIG. 1: (a) Normalized local field intensity  $|\mathbf{E}_{\text{tot}}(\mathbf{r})|^2/|\mathbf{E}_{\text{ext}}|^2$  in the nanostructure with a bow-tie shaped hole, for static ( $\omega = 0$ ) external field. Note strong field enhancement near the sharp edges. (b) Normalized local field intensity  $|\mathbf{E}_{\text{tot}}(\mathbf{r}_0)|^2/|\mathbf{E}_{\text{ext}}|^2$  (solid line) and phase (dashed line) in the center of the nanostructure as a function of photon energy of the external field  $h\nu$ . Note many local extrema due to multiple geometric resonances in the nanostructure. The resonance peak occurs at  $h\nu \approx 0.8$  eV as the phase reaches  $\pi/2$  value.

simulations assuming room temperature  $T = 300$  K  $\approx 25.8$  meV and linearly polarized external field with the polarization direction parallel to the  $x$  axis.

Figure 1(a) shows spatial distribution of the normalized total field intensity  $|\mathbf{E}_{\text{tot}}(\mathbf{r})|^2/|\mathbf{E}_{\text{ext}}|^2$  in the static ( $\omega \rightarrow 0$ ) limit. Note strong field enhancement in the vicinity of the bow-tie sharp edges. We assume that controlled molecule is localized in the center of the hole, in the point of local field maximum, which is our target region.

We performed calculations of the local field  $\mathbf{E}_{\text{tot}}$  in the target region for different frequencies of the external field, Fig. 1(b). Note that the main plasmonic resonance peak occurs at  $\omega \approx 0.8$  eV as the phase reaches  $\pi/2$  value. The frequency dependence has many local extrema due to multiple geometric resonances in the nanostructure. Using the spectral response data of Fig. 1(b), the temporal structure of the local field induced by an arbitrary incident field can be uncovered, Eq. (4), by Fourier transforming the product of the response of the nanostructure and the incident field complex spectrum. Similarly, the external control field in the frequency domain can be computed simply by dividing the given local field complex spectrum by the nanostructure response function.

Some examples are shown in Fig. 2: A 10 fs transform-limited Gaussian pulse, Fig. 2(a,b) incident on the nanostructure will result in a local field shown in Fig. 2(c,d).

Note the substantial difference in the shape of the local field as compared to the incident field, particularly the parasitic “ringing” following the main pulse. This is not surprising, since in the simplest view the collective response of the electrons in the nanostructure comprise a damped oscillator with one or more eigenmodes, the frequencies and amplitudes of which are determined by the geometry and electron concentration. The solution to the inverse problem of obtaining the local field of the form shown in Fig. 2(a,b) is displayed in Fig. 2(e,f) and is easy to understand by noticing that the spectral phase of the incident field is simply the inverted phase of the nanostructure response. Similarly the spectral amplitude structure of the incident field compensates for the spectral variations of the nanostructure response to result in a smooth amplitude spectrum of the local field. A consequence of this is that the “ringing” on the drive pulse is exactly out of phase with the nanostructure “ringing”, so that the two contributions cancel each other.

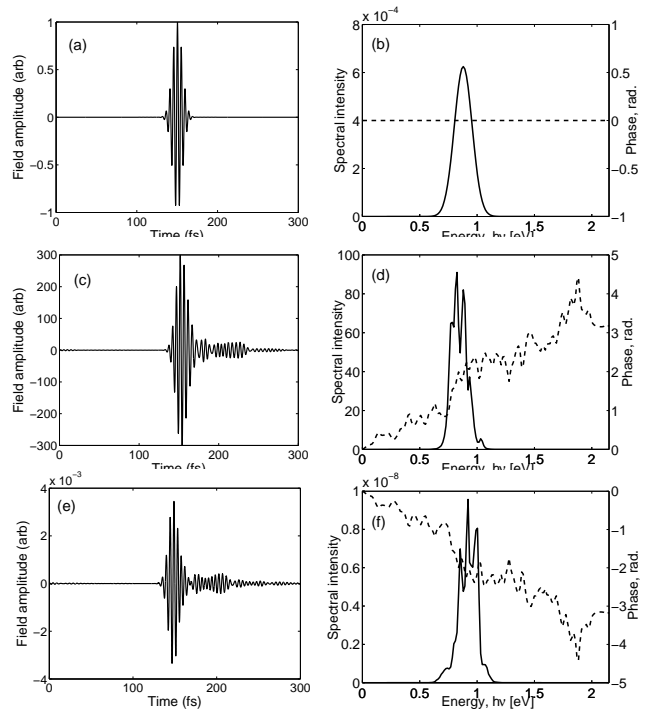


FIG. 2: (a) Time dependence of a Gaussian external field pulse with duration 10 fs. (b) Spectral intensity and phase of the incoming pulse shown in (a). Note, the phase of the pulse is set to zero. (c) Time dependence of the local field excited in the target region by the pulse (a). (d) Spectral intensity and phase of the local field shown in (c). (e) Time dependence of the external field that excites the total field in the target region, same as in (a). (f) Spectral intensity and phase of the incoming pulse shown in (f).

In conclusion, we have demonstrated theoretically the feasibility of optimal coherent control near metallic nanostructures, and how to use the resonant properties of the nanostructure to generate strongly enhanced, spatially *and* temporally localized control field. We have shown that the local field shape deformation and para-

sitic "ringing" can be successfully eliminated. For relatively weak fields one can readily find an external control field, that for the particular geometry and given carrier concentration in the nanostructure will generate the necessary local control field at a given point. The solution of the inverse problem always exists and does not depend on the shape of the optimal local pulse. In practice, the *optimal* control pulse can be found using standard closed loop techniques [17], because the exact response of each given nanostructure will be nearly impossible to measure. Moreover, we studied the frequency dependence of the local field at various points within the nanostructure. Although the inhomogeneous local field amplitude may vary significantly from point to point, we discovered that the phase of the field is much less sensitive to spatial variations. This provides additional tolerance to the position fluctuations of the controlled molecule.

In our simulations we used a model of non-interacting electrons trapped in the nanostructure. Such simplifications will potentially lead to underestimation of the Landau damping [18], resulting in narrower resonance peaks. However, the position of the main resonance peaks obtained, for example, using the *ab initio* Density Functional Theory, should be similar to our simplified model [18]. The applicability of the linear response theory, used in this study, is limited to relatively weak fields. For many optimal control applications this assumption holds. However, in some cases, the field intensity can be high enough, resulting in significant temperature rise and strong nonequilibrium electron distribution [8], which will require the use of the nonlinear response theory. Further, the breakdown of the linear response approximation will make the response kernel  $\hat{\mathbf{Z}}(\mathbf{r}_0, \omega)$  dependent on the amplitude of the external field. In this case one cannot guarantee the inversion of Eq.(4) for an arbitrary optimal local field.

The electron-electron, electron-phonon scattering and other processes, having unpredictable, stochastic nature lead to thermalization of the electron gas in the nanostructure and eventually to the loss of coherence in the system [13]. However, if the controlled molecule is not in the direct contact with the nanostructure, these processes would not limit the possibility of the optimal control. Because of the relatively large number of electrons in the nanostructure, the local electric field has no uncertainties related to the quantum dynamics of electrons, and the nanostructure effectively acts as a *linear filter*. In this case the coherent control is limited by the intrinsic decoherence times of the controlled molecule. However, as we mentioned above, these times may be decreased due to the dynamical screening effects [10].

Since the temporal profile of the local control field keenly depends on the position of the controlled molecule on the nanostructure, one needs to address possible mechanisms and controllability of spatial localization of the controlled molecules. It was theoretically demon-

strated that the plasmon-generated spatially inhomogeneous field between metal nanoparticles can serve as a trap for molecules [19] without direct contact to the nanoparticles, which otherwise would lead to strong decoherence. It was also shown [12, 19] that the field enhancement is maximum in the space between the nanoparticles. Thus, properly arranged arrays of metal nanoparticles may offer *both* trapping and field enhancement capabilities.

This work was performed, in part, at the Center for Integrated Nanotechnologies, a U.S. Department of Energy, Office of Basic Energy Sciences user facility. Los Alamos National Laboratory, an affirmative action equal opportunity employer, is operated by Los Alamos National Security, LLC, for the National Nuclear Security Administration of the U.S. Department of Energy under contract DE-AC52-06NA25396.

- 
- [1] A. P. Peirce, M. A. Dahleh, and H. Rabitz, Phys. Rev. A **37**, 4950, (1988).
  - [2] A. H. Zewail, J. Phys. Chem. A **104** 5660 (2000).
  - [3] A. Assion, T. Baumert, M. Berg, T. Brixner, B. Kiefer, V. Seyfried, M. Strehle, G. Gerber, Science, **282**, 919 (1998).
  - [4] G. Chen, N. H. Bonadeo, D. G. Steel, D. Gammon, D. S. Katzer, D. Park and L. J. Sham, Science **289**, 1906 (2000).
  - [5] V. I. Prokhorenko, A. M. Nagy, S. A. Waschuk, L. S. Brown, R. R. Birge, R. J. Dwayne Miller, Science **313**, 1257 (2006).
  - [6] H. Petek and S. Ogawa, Prog. Surf. Sci. **56**, 239 (1997).
  - [7] H. Petek, S. Ogawa, Annu. Rev. Phys. Chem. **53**, 507 (2002).
  - [8] K. Watanabe, D. Menzel, N. Nilius, and H.-J. Freund, Chem. Rev. **106**, 4301 (2006); C. Frischkorn and M. Wolf, Chem. Rev. **106**, 4207 (2006).
  - [9] M. I. Stockman, D. J. Bergman, and T. Kobayashi, Phys. Rev. B **69**, 054202 (2004).
  - [10] S. Astilean, Rad. Phys. and Chem. **76**, 436 (2007).
  - [11] M. Alducin, J. I. Juaristi, P. M. Echenique, Surf. Sci. **559**, 233 (2004).
  - [12] I. Grigorenko, S. Haas and A.F.J. Levi, Phys. Rev. Lett. **97**, 036806 (2006); I. Grigorenko, S. Haas, A. Balatsky and A. F. J. Levi, New J. Phys. **10**, 043017 (2008).
  - [13] S. Sauvage, P. Boucaud, and T. Brunhes, M. Broquier, C. Crepin, J.-M. Ortega, J.-M. Gerard, Phys. Rev. B, **66** 153312 (2002).
  - [14] A. Kaiser and V. May, Chem. Phys. Lett. **405**, 339 (2005).
  - [15] E. X. Jin and X. Xu, Appl. Phys. Lett. **88**, 153110 (2006).
  - [16] C. Persson, B.E. Serrelius, A. Ferreira da Silva, R. Ahuja and b. Jahansson, J. Phys.: Cond. Matter **13**, 8915 (2001).
  - [17] R. S. Judson and H. Rabitz, Phys. Rev. Lett. **68**, 1500 (1992).
  - [18] A. G. Eguiluz, Phys. Rev. Lett. **51**, 1907 (1983).
  - [19] H. Xu and M. Kall, Phys. Rev. Lett. **89**, 246802 (2002).